Jurnal Kejuruteraan 34(1) 2022: 109-115
https://doi.org/10.17576/jkukm-2022-34(1)-10

An Investigation into the Effect of Backup Coat Sands on Investment Casting Products

Vishal N Kaila[a*] & Indravadan B. Dave[b]

[a]Metallurgy Engineering, Government Polytechnic, Rajkot-360003, Gujarat, Affiliated with Gujarat Technological University, Ahmedabad, Gujarat, India
[b]Metallurgy Engineering Department, Government Engineering College, Gandhinagar-382028, Gujarat, India.

*Corresponding author: vnk.met@gmail.com

Received 4 May 2021, Received in revised form 29 June 2021
Accepted 29 July 2021, Available online 30 January 2022

ABSTRACT

Investment casting is a well-known method for producing precise and finished products. The shell-making process takes a long time and consumes a large amount of coating sands. On the wax pattern tree, the ceramic coating sands are used as a primary coat and several backup coats. Zirconia sand is used for primary coating on a shell in this work. Backup coat sands are made up of fused silica and alumina silica. Colloidal silica is used as a binding material in the formation of all shells. In the work, the effect of fused silica and alumina-silica sand as a backup coat on casting properties was determined. The experimental work evaluated casing properties such as microstructures, grain size measurement, gas porosity, and shrinkages. On the dried, de-waxed, and fired shell, the porosity of the shell mold was determined for the permeability level. Alumina-silica sand has a porosity of 27 to 31 percent, whereas fused silica has a porosity of 22 to 25 percent. It produces better casting properties in alumina–silica casting products than fused silica. Casting grain sizes range from 22 to 38 microns. The grain size of alumina-silica casting is finer than that of fused silica shell casting. Gas porosity and shrinkage in the casting were found to be moderate in all castings.

Keywords: Investment casting; shell mold; backup coat; porosity; shrinkage; permeability

INTRODUCTION

The investment casting process is preferred for producing complex and high-quality products with a smooth surface finish. However, due to the lengthy process time and the use of shell mold materials, the process is not suitable for small-scale production. As a result, it always leads to innovation and development in mold materials for better casting yield and defect reduction (Kumar, Singh, and Ahuja 2015; Kuo et al. 2019). The most common types of casting defects are porosity and shrinkage (Huang, Huang, and Chou 2019). Pattern making, shell making, and molten metal solidification are all part of investment casting. The quality of the casting is determined at each stage. The pattern may influence the dimensional quality of the casting, whereas shell mold materials impart casting properties. It also determines the mechanical properties of molten metal during directional solidification (Liu et al. 2015).

Depending on the size of the casting, a primary coat of zircon dioxide sand is applied, followed by several backup coats of ceramic sand (Amiri Farsani and Gholamipour 2020; Bundy and Viswanathan 2009). Other oxides, such as Alumina, Fused Silica, Yitria, and Calcium oxide, are used as coating sand depending on the type of casting (Cheng et al. 2014). When compared to other oxides, zircon dioxide is used as a primary coating because it is non-reactive and the most stable at high temperatures. (Jia, Cui, and Yang 2006). Because shell making takes a long time because it involves dipping and drying in slurry and consumes a large number of sand materials, it encourages innovation in mold materials and shell making methodology, which reduces the drying time of the shell and improves the shell mold properties (Harun et al. 2009; Li et al. 2019). Permeability is maintained in shell manufacturing by the size and type of ceramic sand used (Kumar and Karunakar 2019). Inadequate permeability results in gas porosity and casting shrinkage

(Pattnaik, Karunakar, and Jha 2012; Yuan and Jones 2003).

Shrinkage is affected by the temperature of the molten metal, the firing temperature of the ceramic shell before pouring, metal solidification, and casting design (Lü, Liu, and Duan 2019). All of these variables influence the dimensional accuracy of the casting (Dong et al. 2017). However, the design alternation, gate location, and runner emphasis on the shrinkage phenomenon have limitations (Tian et al. 2018). The porosity of the shell mold increases during the firing stage after the shell has been de-waxed. Shrinkage appears in the casting as a result of insufficient porosity in the shell mold before pouring molten metal into the shell mold (Kumar and Karunakar 2021).

In this study, four different types of backup coat sand materials were tested to see how they affected casting quality. To understand the micro behavior of the casting, micro examination, and image analysis were performed, while radiography was performed to determine the gas pores and shrinkage level within the cast product. The porosity of the shell has been measured during the shell-making and post-processing stages of the investment casting process. It governs the evolution of the permeability level in the shell mold of an investment casting.

EXPERIMENTAL WORK

SHELL MOLD MAKING AND CASTING

In the present work, Wax patterns were prepared from the die by using a pneumatic injection mold machine. The wax pattern was assembled with a common runner system as shown in Figure 1. Shells were prepared by applying a primary coat and several backup coat sand on the wax pattern assembly. The wax assembly dipped into the silica flour slurry followed by a primary coating of zircon dioxide sand. After that backup coat was applied to the primary coating. The backup coat sand mixture contains Silica (SiO_2) and Alumina (Al_2O_3) in composition as shown in Table 1. There was seven coating layer applied on the primary coat with the same colloidal silica binder. Each coat was allowed to dry for an average of 5 hours, with humidity kept between 70 and 75 percent. Finally, a seal coat was applied and allowed to dry for 48 hours to prevent the degradation of the sand from the final coat. The wax was removed from the shell mold by using the autoclave furnace at the temperature of 150°C. Then de-waxed shell was subjected to firing before casting at the temperature of 1000°C for 60 minute.

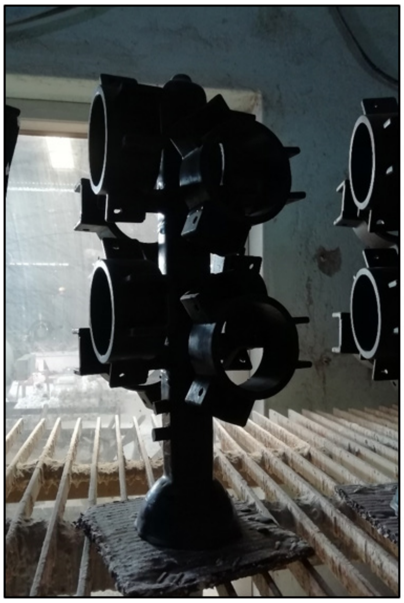

Figure 1. Wax pattern assembly

Table 1. Details of backup coat materials

Sr.	Coding of Material	Source of backup coat sand	Composition in wt. %			Cost of Sand (Rs. per kg.)
			SiO_2	Al_2O_3	Other oxides	
1	FSS	Fused silica sand	100	--	--	75.00
2	CSW	Ceramic Sanitary waste	63	33	4	8.00
3	CTW	Ceramic Tile waste	66	23	11	6.00
4	FRW	Furnace refractory waste	44	47	9	6.50

Commercially available mild steel raw metal was used to produce the casting. The composition of WCB grade cast steel was; 0.17% C, 0.30% Si, 0.34% Mn, 0.015% S, and 0.04% P. Mild steel was melted at a temperature of 1550°C in an induction furnace. Molten metal was poured into the fired shell to make the casting. Then casting allowed to solidify and knock off the shell by the vibratory table. The cut-off operation was carried out to separate the casting product from the runner and gates. The casting product design is shown in Figure 2.

Figure 2. Cast product in as-cast condition

SHELL POROSITY MEASUREMENT

The porosity was measured as per the IS 13630 (2006, Part-2) at the Central Glass and Ceramic Research Institute (CSIR). The shell mold samples were immersed in the water and weighed with absorbed water by each sample. Samples were dried off in the oven at the temperature of 110°C for 24 hours. Cooled samples were reweighed after removing water completely from the samples. Porosity is proportionate to the water absorbed in the porous mass of the mold. It was calculated as per Equation 1 in the form of a percentage.

$$P = \frac{m_2 - m_1}{m_1} \times 10 \qquad \text{… Eq. (1)}$$

Where, m_1 is the mass of the dry samples in gm and m_2 is the mass of the wet samples in gm.

MICRO EXAMINATION AND IMAGE ANALYSIS

The phase distribution and image analysis were carried out for the as-cast product. The microstructure was observed under an optical microscope (Olympus GX41) at the Devine metallurgical services laboratory. The microstructure was prepared and etched with 2% Nital sol. Micro images were observed at 100X magnification.

Phase identification and distribution were carried out as per the ASTM E-562 method by Optical microscope (BMI 1000X). Image analysis was performed by the same microscope at the standard magnification of 100X. The grain size of the as-cast component was determined as per the ASTM E-112 method.

NON-DESTRUCTIVE TEST

The radiography non-destructive test was performed on the cast product to identify the gas porosity and shrinkage defects. A radiography test was carried out as per ASME section 5, articles 2 and 22 at the Radio Tech NDT Laboratory. The radiographic images were taken in the position A, B, C and DE on the casted product. The casting product shape is given in Figure 2, the casting product has three faces, so each face has been identified as position A, B, and C, while the top surface of the casting tested under position DE as per Figure 3.

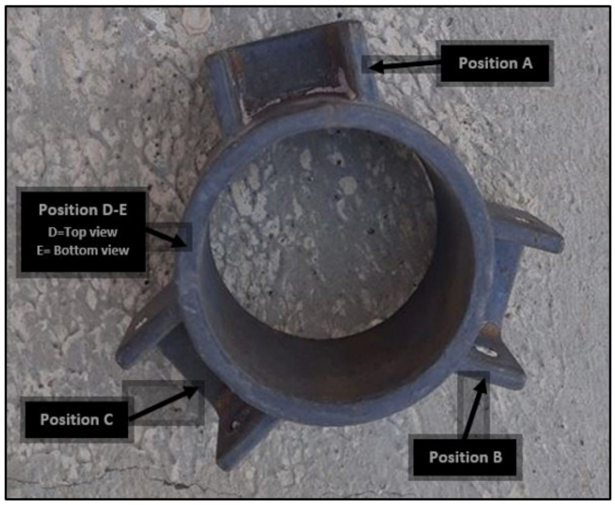

Figure 3. Position on casting product for radiography test

RESULTS AND DISCUSSIONS

In the present research work, results are presented in the form of graphics and images with detailed interpretation.

POROSITY OF SHELL MOLD

Figure 4 shows the porosity present across the shell mold. It reveals the porosity level increase after de-waxing and firing the shell. Gating system design restricts the permeability development in the shell. It can be resolve by firing the shell at 1000°C temperature, which develops sufficient permeability into the shell. The Fused silica sand shows a low porosity compared to the alumina-silica sand type shell. Furthermore, other oxides present in the composition enhance the porosity development. The porosity of the shell proportionates to the permeability, so the casting quality can be improved by controlling the porosity of the shell mold.

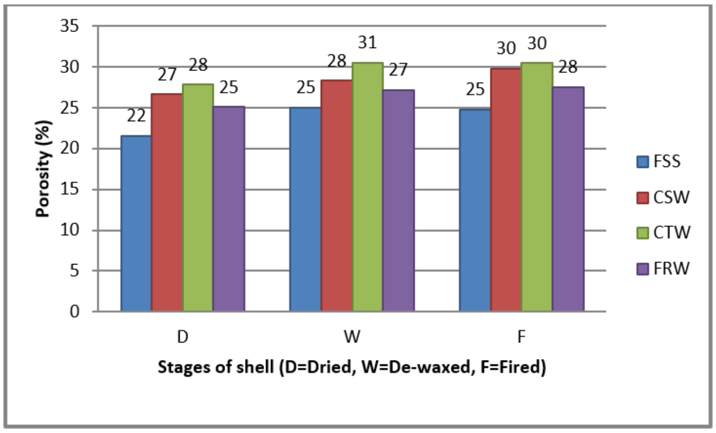

Figure 4. Porosity results of shell mold

MICRO ANALYSIS

The microstructure of the as-cast mild steel sample is as shown in Figure 5. It revealed the ferrite and pearlite phases in the images. The phases are uniformly distributed among the structure. Furthermore, there are no uni-axed grains found in the structure as it was taken as-cast without heat treatment.

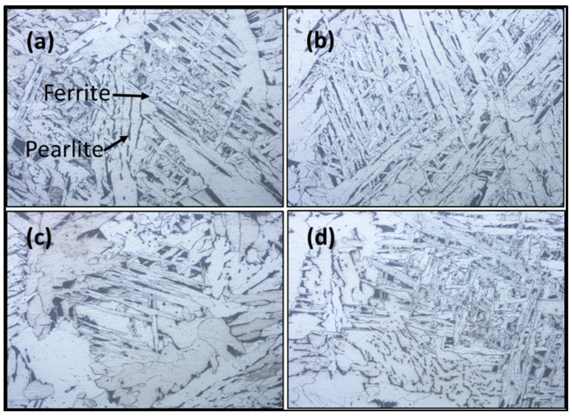

Figure 5. Microstructure of cast products (a) FSS sand (b) CSW sand (c) CTW sand (d) FRW sand

As per Table 2, Image analysis results show the quantitative distribution of pearlite and ferrite phases in the structure. Mainly pearlite phase varies with the percentage of carbon in the composition of the mild steel. FSS type reveals more pearlite compare to other shell types since FSS consists of 100% fused silica in composition.

Table 2. Phase analysis results by image analyzer

Product	Phase analysis		Hardness in HV
	Ferrite (%)	Pearlite (%)	
FSS	79	21	124
CSW	85	15	131
CTW	82	18	121
FRW	86	14	127

Grain size measurement results are shown in Table 3. The grain size of casting varies from 22 to 31.8 microns. FRW types develop fine grains in structure compare to the FSS type, while CSW and CTW types show similar and moderate grain sizes. This result indicates that the shell porosity directly affects the development of the microstructure of casting. An adequate porosity of the shell provides a better heat exchange and result in a fine grain structure of casting, it can improve the mechanical properties of the casting.

Table 3. Grain size of phases in the microstructure

Product	Grain Size Analysis	
	Grain Size Number	Grain Size in micron
FSS	7-7.5	26.7-31.8
CSW	7.5	26.7
CTW	7.5	26.7
FRW	8	22.5

GAS POROSITY AND SHRINKAGES

Table 4 shows the shrinkages and gas pores present in the casting produced by different types of backup coat sands. Radiography film developed to find out the gas porosity level as shown in Figure 6. It is observed that gas pores present in the casting of levels 1 and 2. Shrinkage was found in casting at a moderate level of 3 (CB-III). Feathery-type shrinkage was observed in all types of castings. FSS shows the presence of gas pores and shrinkage in the casting. The porosity of the shell mold affects the permeability at the time of solidification, so results in gas porosity. CTW and CSW type casting shows moderate feathery type shrinkage in the castings. In general, castings contain the minimal formation of gas porosity, while shrinkages are observed at a moderate level.

Table 4.Shrinkages and Gas porosity in the cast products

Shell type	Radiography film position on component			
	A	B	C	DE
FSS	--	--	A-II	CB-III
CSW	CB-III	CB-III	--	--
CTW	CB-III	--	CB-III	--
FRW	--	CB-IV	--	CB-II, A-I

*CB- Feathery shrinkage A-Gas porosity

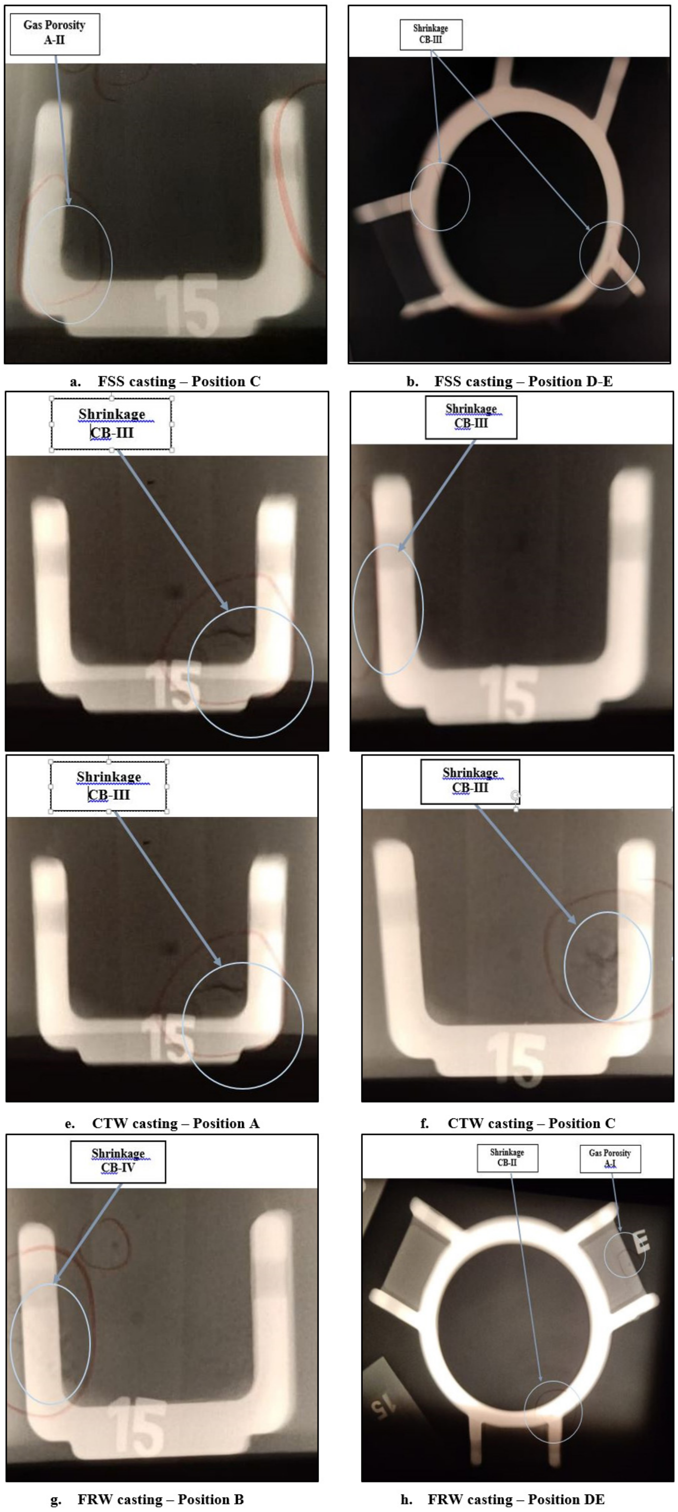

Figure 6. Radiography films for gas porosity and shrinkage defects

CONCLUSIONS

In this work, the fused silica-based (FSS) and alumina-silica-based (CSW, CTW, and FRW) type backup coat sand use to show the effect on the properties of the casting product. Based on the results following conclusions can be drawn.

1. Alumina-silica type sand shows the feasibility to use as backup coat sand as it is the ceramic waste. So it provides the near results to the fused silica with the cost-effective (Table 1) production.

2. The porosity of the shell mold increase in the stage of the firing before pouring. The FSS type shows low porosity 22 to 25% in the shell compares to alumina-silica type 27 to 30% porosity.

3. Microanalysis of the cast product reveals the fine grain size of 22 microns in the FRW type and coarser grain size of 26.7 to 31.8 microns in the FSS type. It shows the effect of porosity on the solidification of the casting.

4. Shrinkages and Gas pores defects found the marginal increase severity level 5 and 18 respectively in the fused silica than alumina-silica typecasting.

Overall concluded that the waste ceramic backup coat sand can be used as an alternative to fused silica since the providing near about results in the casting with lower cost.

ACKNOWLEDGEMENT

The authors are highly thankful to Gujarat Technological University and Government Engineering College on its excellent help and support to conduct this research.

DECLARATION OF COMPETING INTEREST

None.

REFERENCES

Amiri Farsani, Maryam, and Reza Gholamipour. 2020. Silica-free zirconia-based primary slurry for titanium investment casting. *International Journal of Metalcasting* 14(1):92–97. doi: 10.1007/s40962-019-00335-y.

Bundy, J., and S. Viswanathan. 2009. Characterization of zircon-based slurries for investment casting. *International Journal of Metalcasting* 3(1):27–35. doi: 10.1007/bf03355439.

Cheng, X., C. Yuan, S. Blackburn, and P. A. Withey. 2014. The study of the influence of binder systems in an Y2O3-ZrO2 facecoat material on the investment casting slurries and shells properties. *Journal of the European Ceramic Society* 34(12):3061–68. doi: 10.1016/j.jeurceramsoc.2014.03.005.

Dong, Y. W., X. L. Li, Qi Zhao, Jun Yang, and Ming Dao. 2017. Modeling of shrinkage during investment casting of thin-walled hollow turbine blades. *Journal of Materials Processing Technology* 244:190–203. doi: 10.1016/j.jmatprotec.2017.01.005.

Harun, Z., D. T. Gethin, R. W. Lewis, and W. J. Ferguson. 2009. Drying of a multilayer ceramic shell body. Proceedings of the Fifteenth UK Conference of the Association of Computational Mechanics in Engineering 85(April 2007). doi: 10.4203/ccp.85.16.

Huang, Pei Hsing, Wei Ju Huang, and Chuen Shii Chou. 2019. Preventing casting defects of stainless steel flanges using a water-soaking method. *Materials Science Forum 962 MSF* (August):189–93. doi: 10.4028/www.scientific.net/MSF.962.189.

Jia, Q., Y. Y. Cui, and R. Yang. 2006. A study of two refractories as mold materials for investment casting TiAl based alloys. *Journal of Materials Science* 41(10):3045–49. doi: 10.1007/s10853-006-6785-3.

Kumar, Parlad, Rupinder Singh, and I. P. S. Ahuja. 2015. Investigations on dimensional accuracy of the components prepared by hybrid investment casting. *Journal of Manufacturing Processes* 20:525–33. doi: 10.1016/j.jmapro.2015.07.008.

Kumar, Sanjay, and D. Benny Karunakar. 2019. Enhancing the permeability and properties of ceramic shell in investment casting process using ABS powder and needle coke. *International Journal of Metalcasting* 13(3):588–96. doi: 10.1007/s40962-018-00297-7.

Kumar, Sanjay, and D. Benny Karunakar. 2021. Characterization and properties of ceramic shells in investment casting process. *International Journal of Metalcasting* 15(1):98–107. doi: 10.1007/s40962-020-00421-6.

Kuo, Jenn Kun, Pei Hsing Huang, Hsin Yi Lai, and Wei Jen Wu. 2019. Design of casting systems for stainless steel exhaust manifold based on defective prediction model and experimental verification. *International Journal of Advanced Manufacturing Technology* 100(1–4):529–40. doi: 10.1007/s00170-018-2737-8.

Li, Yanfen, Xiangdong Liu, Kai Lű, and Xiaodong Du. 2019. Preparation of fiber-reinforced shell by airflow placement fiber technology for investment casting. *International Journal of Metalcasting* 13(4):979–86. doi: 10.1007/s40962-019-00323-2.

Liu, Changhui, Sun Jin, Xinmin Lai, Bo He, and Fei Li. 2015. Influence of complex structure on the shrinkage of part in investment casting process. *International Journal of Advanced Manufacturing Technology* 77(5–8):1191–1203. doi: 10.1007/s00170-014-6523-y.

Lü, Kai, Xiangdong Liu, and Zehai Duan. 2019. Effect of firing temperature and time on hybrid fiber-reinforced shell for investment casting. *International Journal of Metalcasting* 13(3):666–73. doi: 10.1007/s40962-018-0280-x.

Pattnaik, Sarojrani, D. Benny Karunakar, and P. K. Jha. 2012. Developments in investment casting process - A review. *Journal of Materials Processing Technology* 212(11):2332–48. doi: 10.1016/j.jmatprotec.2012.06.003.

Tian, Guo liang, Kun Bu, Dan qing Zhao, Ya li Zhang, Fei Qiu, Xian dong Zhang, and Shuai jun Ren. 2018. A shrinkage prediction method of investment casting based on geometric parameters. *International Journal of Advanced Manufacturing Technology* 96(1–4):1035–44. doi: 10.1007/s00170-018-1618-5.

Yuan, C., and S. Jones. 2003. Investigation of fibre modified ceramic molds for investment casting. *Journal of the European Ceramic Society* 23(3):399–407. doi: 10.1016/S0955-2219(02)00153-X.